Mössbauer analysis of ultrathin ferromagnetic Fe(110) films on W(110) coated by Ag

M. Przybylski,* I. Kaufmann, and U. Gradmann
Physikalisches Institut, Technische Universität Clausthal, D-3392 Clausthal-Zellerfeld, Federal Republic of Germany and Sonderforschungsbereich 126 Göttingen/Clausthal of the Deutsche Forschungsgemeinschaft D-3392 Clausthal-Zellerfeld, Federal Republic of Germany
(Received 30 January 1989)

Conversion-electron Mössbauer spectroscopy of ultrathin pure ^{57}Fe(110) films on W(110) coated by Ag provides detailed information on the mode of growth, the film structure, and the local structure of magnetic order, in particular its thermal decrease, because different structural components are marked by strongly differing magnetic hyperfine fields.

I. INTRODUCTION

The local structure of magnetic order forms a basic problem of ultrathin ferromagnetic films. For the ground state, strong inhomogeneities have been predicted recently by self-consistent band-structure calculations[1] both for magnetic moments per atom and for magnetic hyperfine fields. For finite temperatures, the inhomogeneities of the thermal decrease of magnetic order have been analyzed in theory many years ago in ultrathin Fe films.[2] Experimental analysis faces two problems: First of all, films grown layer-by-layer, down to the monolayer, which form the subject of theoretical analysis, must be prepared and checked by appropriate methods, and second, magnetic order must be analyzed in them by an appropriate local probe. In principle, Mössbauer spectroscopy provides this local probe of magnetic order, via magnetic hyperfine fields B_{hf}. The aim of this paper is to show how conversion-electron Mössbauer spectroscopy (CEMS) of Fe(110) films on W(110) coated by Ag provides combined information on both the local structure of magnetic order and the film structure in the monolayer regime.

One mode of the local Mössbauer analysis in Fe films is based on samples containing only one probe layer of the Mössbauer isotope ^{57}Fe; the rest of the film consists of ^{56}Fe. In the first application of this principle to Fe(110) films on Ag(111)[3] using transmission Mössbauer spectroscopy, monolayer probes could not be used because of signal-to-noise problems. Only by using the more sensitive CEMS technique *in situ* in ultrahigh vacuum (UHV's)[6] could monolayer resolution be realized and local oscillations of B_{hf} be observed near the free surface of relatively thick Fe(110) films on W(110), which consisted of 21 atomic layers. A similar analysis of the Fe(110)/W(110) interface[7] was complicated by some intermixing between the ^{57}Fe probe layer and neighboring ^{56}Fe layers, caused by the periodic misfit dislocation in this misfitting interface ($f_{Fe/W}=-9.4\%$). However, the local analysis was facilitated by the fact that B_{hf} in the first Fe(110) layer on W(110) is reduced to 23 T (in the ground state, in comparison with 34 T in bulk). An even stronger reduction to 12 T was recently observed for a monolayer of Fe(110) on W(110), as it was coated by Ag.[8] This strong difference of B_{hf} for different structural components is used in this paper for the local analysis of ultrahin Fe(110) films on W(110) in the monolayer regime. We will show how, in properly prepared pure ^{57}Fe films, different structural components can be identified by their different values of B_{hf} much easier than in a similar analysis of Fe(110) on Ag(111),[9] because of the much stronger differences in B_{hf}. We will further show how, by using this identification via B_{hf}, the relative contributions of structural components can be determined in the growing film, and their comparison with simple model predictions results in valuable structural information.

A related CEMS analysis of Fe(110)/Ag(100) multilayers[10] recently showed relaxation broadening of the lines, indicating a fine-grained structure in the monolayer regime, in accordance with the surface energies [$\gamma_{Fe}=2.0$ J m^{-2}, $\gamma_{Ag}=1.1$ J m^{-1} (Ref. 11)], which indicate a nonwetting condition.[12,13] Conversely, for Fe(110) on the high-surface-energy substrate W(110) ($\gamma=2.9$ J m^{-2}), nucleation by a thermodynamically stable monolayer was established recently,[14] in agreement with previous low-energy electron diffraction–Auger-electron spectroscopy (LEED-AES) analysis of Fe(110) on W(110).[15,16] Accordingly, we observed sharp spectra without any indication of relaxation broadening in all films of the present study. In combination with LEED and AES we will show that a pseudomorphic double layer can be formed at 300 K and further layer growth can be realized to a good approximation.

The paper is organized as follows: After describing the experimental methods in Sec. II, the main body of the CEMS experiments is presented in Secs. III A, III B, and III C, presenting three series of films. The film series of Sec. III A was prepared at 300 K and CEMS spectra were taken at 300 K as a function of film thickness; because layer growth occurs at these conditions, the spectra can serve for a straightforward unique attribution of spectral to structural components. Films of Sec. III B, prepared at 475 K, show sensitive reaction of film structure on growth conditions and sensitive detection of deviating structures by CEMS. Finally, temperature-dependent spectra are presented in Sec. III C for a series of films consisting of integer numbers of atomic layers. Comple-

mentary LEED AES experiments are presented in Sec. IV. The concluding discussion of Sec. V starts with film structure and mode of growth, followed by a discussion of magnetic hyperfine fields and their temperature dependence, which represents the dependence of magnetic order. This paper is based on previous work on the ferromagnetic monolayer.[8,14,17] Submonolayer films are not included; they are planned to be reported elsewhere.

II. EXPERIMENT

Experiments were performed using a previously[5] described CEMS spectrometer, working *in situ* in UHV. The UHV system ($p<3\times10^{-11}$ Torr) is equipped for molecular-beam epitaxy (MBE) of different metals, including the pure Mössbauer isotope ^{57}Fe and Ag. Pure ^{57}Fe films were prepared at $p<10^{-10}$ Torr with growth rates of 2–4 Å/min on W(110) substrates. Film thickness was measured using quartz oscillators with an accuracy of ±5% of one monolayer Fe. For Mössbauer analysis, films were irradiated by γ rays from a small area moving the ^{57}Co-Rh source, operating outside the vacuum system, through a Be window, at grazing incidence (grazing angle $\approx15°$) in the [1$\bar{1}$0] azimuth. Conversion electrons were detected by a combination of a spherical condenser spectrometer, used as an energy filter for the 7.3 keV conversion electrons, and a channeltron multiplier. Mössbauer spectra could be taken at measuring temperatures $T_m\geq90$ K. Using a 100-mCi source, one spectrum of a monolayer took roughly one day. Fe films were routinely tested by LEED after preparation and coated immediately by Ag to prevent residual gas contamination. A supplementary LEED AES analysis of growth modes using the same preparation conditions was done in a separate UHV system, with a four-grid LEED optics both for LEED and for AES analysis in the retarding field mode.

III. MOSSBAUER ANALYSIS

A. Films prepared and coated at 300 K

The first series of films was prepared at $T_{Fe}=300$ K and coated by Ag at $T_{Ag}=300$ K. CEMS spectra of films from this series, taken at a measuring temperature $T_m=295$ K, are presented in Fig. 1, with the number D of bulk monolayers contained in the film as a parameter. Note that because of the misfit $f_{Fe/W}=-9.4\%$ ($a_{Fe}=2.866$ Å; $a_W=3.165$ Å), the pseudomorphic monolayer corresponds to $D=0.82$. All spectra were fitted as a superposition of one nonmagnetic single-line component and four magnetic six-line components, which are indicated by fingerprints. In one six-line component, the position of the lines $(m_{I,e};m_{I,g})=(\frac{3}{2};\frac{1}{2})$; $(\frac{1}{2};\frac{1}{2});(\frac{1}{2};-\frac{1}{2});(-\frac{1}{2};\frac{1}{2});(-\frac{1}{2};-\frac{1}{2});(-\frac{3}{2};-\frac{1}{2})$ were fitted in the standard way[18] by

$$v=\frac{c}{h\nu_0}[-\mu_N B_{hf}(g_{N,e}m_{I,e}-g_{N,g}m_{I,g}) +(-1)^{|m_{I,e}|+1/2}\epsilon+\delta]\,, \quad (1)$$

where v is the velocity of the moving source, directed towards the sample, c is the velocity of light, $h\nu_0=7.3$ keV is the photon energy, μ_N is the nuclear magneton, B_{hf} is the hyperfine field at the ^{57}Fe nucleus, $g_{N,e}$, $g_{N,g}$, $m_{I,e}$, and $m_{I,g}$ are nuclear Landé factors and magnetic quantum numbers in the excited and the ground states, respectively, ϵ is the quadrupole splitting, and δ is the isomer sift, taken with respect to bulk Fe. As in our previous analysis of Fe(110) interfaces,[4] rotational symmetry of the electric-field-gradient tensor with respect to the surface normal was assumed. This approximation was justified both by the fact that we could fit the spectra using it and by an estimate of the symmetry given previously.[4] We have previously shown[19] that Ag-covered Fe(110) films on W(110) are magnetized along [1$\bar{1}$0], below $D=30$, as a result of strong in-plane magnetic surface anisotropies.

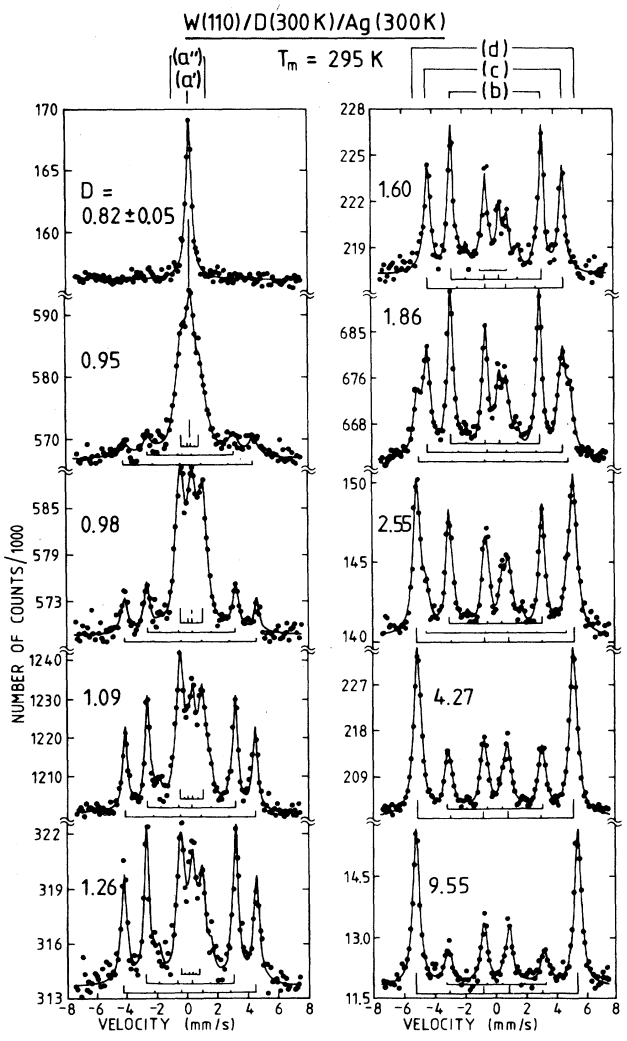

FIG. 1. Mössbauer spectra of Fe(110) films consisting of ($D\pm0.05$) bulk atomic layers of pure ^{57}Fe, prepared on W(110) at $T_{Fe}=300$ K, coated by Ag at $T_{Ag}=300$ K. The spectra were measured at $T_m=295$ K. They were fitted by one single line (a') and four sextets [(a''), (b), (c), and (d)], with relative intensities as indicated by the fingerprints.

We have further shown that for the present geometry (grazing incidence under 15° in the [1$\bar{1}$0] azimuth with angular dispersion of the γ rays as discussed previously[19]), the relative intensities of the six lines are given to a good approximation by

$$I_1:I_2:I_3:I_4:I_5:I_6 = 2.7:0.3:1:1:0.3:2.7 \ ;$$

this ratio was used fixed in the present analysis. Note that because of the dominating magnitude of I_1 and I_6, the components are represented in the spectra mainly by these outer lines; they are indicated by fingerprints in Fig. 1. Hyperfine fields $B_{\mathrm{hf},i}$ and relative contributions p_i of the components $i = a$, b, c, and d, which were used as free parameters of the computer fit, are presented in Figs. 2(a) and 2(b), respectively. We renounce a representation of ϵ and δ, which are small ($0 \le \delta \le 0.15$ mm/s; $|\epsilon| < 0.2$ mm s^{-1}) and not informative in the context of this paper. Strictly speaking, the parameters p_i are relative intensities of the different spectral components. Based on the assumption of a common recoilless fraction, they are interpreted as relative contributions of four structural components as follows (compare Figs. 1 and 2).

(a) From our previous analysis of the ferromagnetic, Ag-coated monolayer,[8,14] we know that its Curie temperature $T_{c,\mathrm{mono}}$ is slightly below room temperature, that for preparation at $T_{\mathrm{Fe}} = 300$ K, $T_{c,\mathrm{mono}}$ can be increased above room temperature by increasing D above 0.82, and that just below $T_{c,\mathrm{mono}}$ the monolayer spectrum forms a superposition of a nonmagnetic single line and a weakly magnetic sextet, with a magnetic hyperfine field B_{hf} of about 4 T just below $T_{c,\mathrm{mono}}$. Accordingly, in this study a monolayer component (a) was expected and detected, consisting just above $D = 0.82$ of a nonmagnetic single-line subcomponent (a') and a weakly magnetic subcomponent (a'') with $B_{\mathrm{HF}} \approx 4$ T, at room temperature.

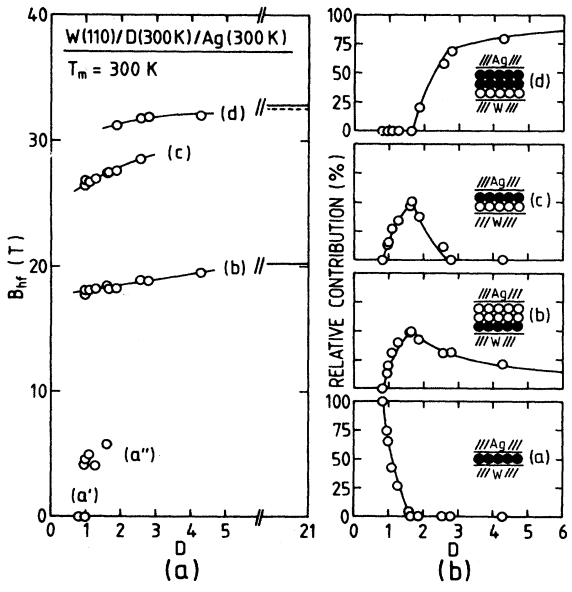

FIG. 2. Fitting parameters for spectra from Fig. 1. (a) Magnetic hyperfine fields B_{hf}. At the right borderline, values from "thick" films ($D = 21$) are given, taken from 7. For component (d), values for the first Fe layer near Ag (— — —) and for the center of the $D = 21$ film (——) are given separately. (b) Relative contributions of components $(a) = (a') + (a'')$, (b), (c), and (d). The structural interpretation of the components is indicated [^{57}Fe atoms (●); ^{56}Fe atoms (○)]. Theoretical predictions from a layer-growth model, starting with two pseudomorphic monolayers (completed at $D = 1.64$), followed by further layers with bulk density, are given by solid lines, for comparison.

(b) In our previous analysis of the Fe(110)/W(110) interface,[7] we showed that in the first Fe (110) layer on W(110) B_{hf} is reduced to 20 T (at room temperature) in comparison with 33 T in bulk. Accordingly, an "interface" component (b) with $B_{\mathrm{hf}} \approx 20$ T was expected and detected in our films, too.

(c) Besides the obvious components (a'), (a''), (b), and (d) (below), one additional component (c) was definitely needed to fit the spectra, with a hyperfine field near $B_{\mathrm{hf}} = 28$ T, as can be seen most clearly from the film $D = 1.86$, where both components (c) and (d) can be identified by visual inspection. Component (c) could be attributed to Fe atoms in the second atomic layer, when coated by Ag, compare Fig. 2(b).

(d) From our previous analysis of the Ag-coated Fe (110) surface,[4,5] we know that at room temperature the hyperfine field near the Ag-coated surface deviates by less than 1 T from the bulk value of 33 T. Accordingly, a "bulklike" component (d) with $B_{\mathrm{hf}} \approx 33$ T was expected and detected, representing all further material, including the Ag-covered surface.

Of course, the fitting procedure cannot be justified by these considerations only. Its justification is given by the dependence of hyperfine fields $B_{\mathrm{hf},i}$ and relative contributions p_i of the components $i = a$, b, c, d, on D, which can be followed qualitatively by visual inspection of the spectra and fingerprints in Fig. 1 or, more clearly, from their direct representation in Fig. 2. Note first that all hyperfine fields $B_{\mathrm{hf},i}$ are smooth, slowly shifting functions of D [Fig. 2(a)]. *All spectra could be fitted by the same set of B_{hf} values* which proves them to be properties of structural components commonly present for all values of D. The definite confirmation of the fitting procedure, however, is given by the relative contributions in Fig. 2(b) and their agreement with the solid lines, which are theoretical predictions from the most simple growth model, in which the film starts by one pseudomorphic monolayer ($D = 0.82$), followed by a second pseudomorphic monolayer, completed at $D = 1.64$, and further layers with bulk density. For example, p_a equals 1 up to $D = 0.82$ (experience from previous monolayer work[8,14,17]), decreases with increasing D, and disappears at $D = 1.64$; components (b) and (c) start at $D = 0.82$, are maximum for the pseudomorphic double layer ($D = 1.64$), and then decrease, component (c) disappearing near $D = 2.64$, where the second monolayer is coated by a third, bulklike one. Obviously the experimental points follow the predictions of the layer-growth model, in the limits of accuracy, given roughly by ±5% both for p_i and D.

As seen from the fingerprints in Fig. 1, the monolayer component (a) changes from the nonmagnetic subcomponent (a') for $D \le 0.82$ (which was observed for several submonolayer films, not included in Fig. 1) to the mag-

netic subcomponent (a'') for $D \geq 1.09$. This is reasonable: The monolayer patches are magnetized by the neighboring double-layer patches, which are ferromagnetic at room temperature. Further confirmation for this interpretation of the spectral components (a') and (a'') as subcomponents of one single structural monolayer component (a) is given in Fig. 3 by the spectra of a film $D=1.16$ prepared at 300 K, measured at different temperatures $T_m=90$, 295, and 345 K, respectively. In addition to the strongly magnetic components (b) and (c), which are observed at all temperatures, we observe a central component (a) which is nonmagnetic (a') at 345 K and becomes weakly magnetic at 295 K [(a''), ($B_{\rm hf}\approx 4$ T)] and stronger magnetic at 90 K ($B_{\rm hf}\approx 11$ T). The relative contributions, however ($p_{a'}=38\%$ at 345 K, $p_{a''}=41$ and 39 % at 295 and 90 K, respectively), agree in the limits of accuracy with the theoretical value $p_a=(1.64-D)/D=41\%$. Both subcomponents obviously represent the monolayer, which is nonmagnetic at elevated temperatures and becomes ferromagnetic near room temperature, as shown previously.[8,14]

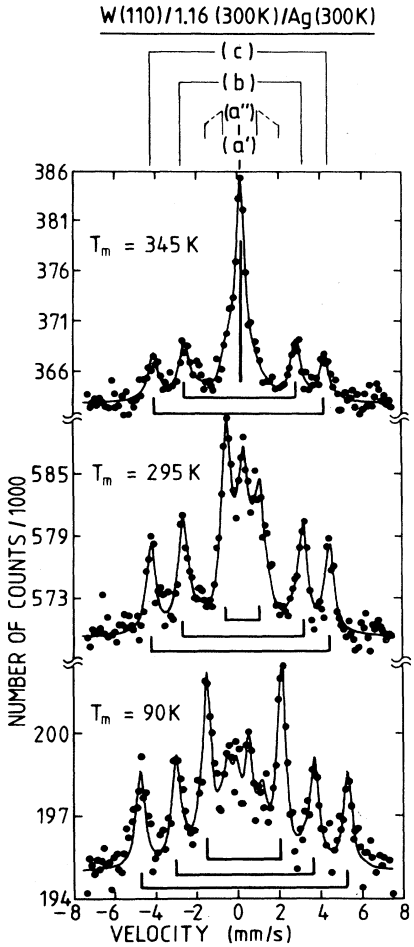

FIG. 3. Mössbauer spectra of a film consisting of $D=1.16$ bulk monolayers, prepared and coated by Ag at 300 K, measured at different temperatures T_m. Component (a), which is nonmagnetic (a') at $T_m=345$ K, becomes magnetic (a'') at $T_m=295$ and 90 K, respectively.

The excellent fit of the experimental results to the layer-growth model in Fig. 2(b) unresistingly confirms both our attachment of spectral to structural components and the presence of layer-by-layer growth up to $D=2.64$ (three layers), including the formation of a pseudomorhpic double layer at $D=1.64$. This is confirmed by the LEED patterns observed for the films of Figs. 1 and 2: For $D\leq 1.64$, the $p(1\times 1)$ pattern of W(110) was observed, indicating pseudomorphic films, for $D>1.64$ the two-dimensional superstructure multiplets indicating interface dislocations.[15] However, the contrast of the LEED pattern was reduced in comparison with preparations at 500 K (Ref. 15) or 475 K (Sec. III B, below), indicating some degree of local disorder for $T_{\rm Fe}=300$ K. For further confirmation of this growth model compare the LEED AES analysis given in Sec. IV.

B. Films prepared at 475 K

In previous work[15] on epitaxial growth of Fe(110) on W(110) it has been shown that a clear LEED pattern with low background, at the surface of thick films, could be realized for preparation temperatures above 200 °C only. We therefore prepared a second series of Fe films at $T_{\rm Fe}=475$ K. They were coated by Ag at the same temperature, $T_{\rm Ag}=475$ K. Mössbauer spectra were measured at $T_m=90$ and 295 K, repsectively. Spectra of these films, taken at $T_m=295$ K, showed dramatic changes in comparison with that of films prepared at 300 K, e.g., the spectrum of a film $D=1.73$ given in Fig. 4, to be compared with spectra for $D=1.60$ and 1.86 in Fig. 1. As a result of the increased preparation temperature, we observed a strong increase of the bulklike component (d), connected with some increase of the monolayer component (a) and a decrease of component (c) (second layer in double-layer patches). Apparently, some recrystallization into thicker crystallites sitting on the first pseudomorphic layer results from the enhanced preparation temperature. In general, this strongly changed microstructure can be recognized from the relative contributions, given in Fig. 5(b) by open circles (○). For $1<D<3$, strong deviations from the layer-to-layer predictions (solid curves) indicates considerable deviations from the ideal structure and recrystallization into thicker crystallites. The monolayer contribution p_a is increased, in comparison with the layer-growth model, and persists up to $D=2.5$; near the pseudomorphic double layer, $D=1.64$, a great deal of atoms is transferred from the second-layer component (c) to the bulklike component (d). However, the sum of the first-layer contributions, p_a+p_b, which is shown in Fig. 6 as a function of P, remains at $p_a+p_b=0.82/D$, as predicted by nucleation from a stable pseudomorphic monolayer. Obviously, the first pseudomorphic monolayer remains stable, and the considerable recrystallization takes place in the following layer only. For further clarification of the driving force of this recrystallization, some films were prepared at $T_{\rm Fe}=475$ K but coated by Ag at $T_{\rm Ag}=300$ K, which left the films of the first series undisturbed, similar to Fig. 2(b). Obviously, these films coated at 300 K (⊗) deviate less from the layer-growth prediction than the films coat-

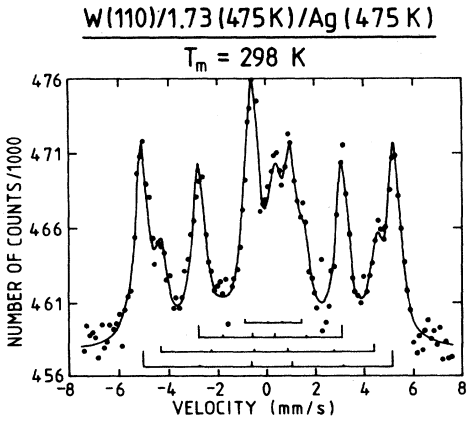

FIG. 4. Mössbauer spectrum of a Fe (110) film of 1.73±0.05 bulk atomic layers of pure ^{57}Fe, prepared on W(110) at T_{Fe}=475 K coated by Ag at T_{Ag}=475 K. The spectrum was measured at T_m=295 K (to be compared with spectra D=1.60/1.86 in Fig. 1).

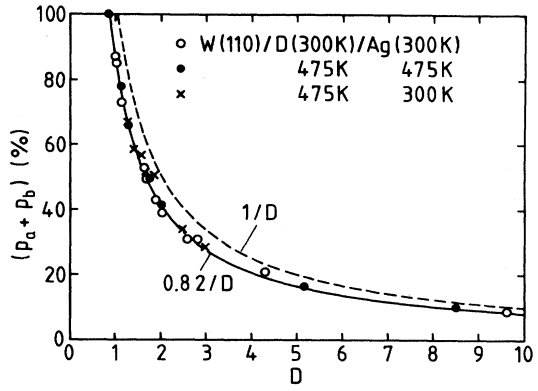

FIG. 6. Relative contribution of monolayer components, p_a+p_b, versus D, for Fe(110) films consisting of D bulk atomic layers for different temperatures T_{Fe} for Fe preparation and T_{Ag} coating; (T_{Fe};T_{Ag})=(300 K;300 K) (○); (475 K;475 K) (●); (475 K;300 K) (×), respectively. Theoretical hyperbolae (p_a+p_b) =1/D (bulk density, — — —) and (p_a+p_b)=0.82/D (pseudomorpic monolayer, ——), for comparison.

ed at 475 K (○): The recrystallization is reduced, but not eliminated. We suppose that the recrystallization is connected with the instability of the second pseudomorphic monolayer, which can be maintained at 300 K as a metastable structure only. This metastability is in accordance with theoretical stability considerations[20] for the case of anharmonic pair interactions. Apparently, the atomic rearrangements in the second and further layers are induced to some minor degree by preparation at 475 K, and they are further promoted by Ag coating at the same elevated temperature. This picture is supported by the LEED AES analysis given below in Sec. IV.

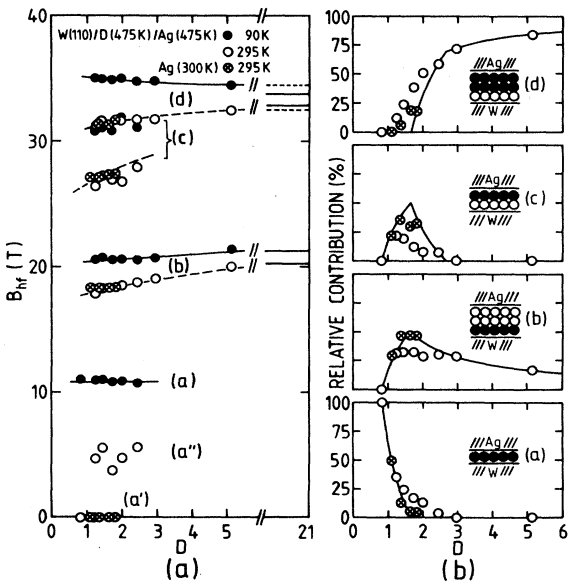

FIG. 5. Fitting parameters of spectra from pure ^{57}Fe(110) films, prepared at T_{Fe}=475 K, coated by Ag at T_{Ag}=475 K (●,○) or 300 K (⊗), respectively, measured at T_m=295 K (○,⊗) or 90 K (●), respectively. (a) Magnetic hyperfine fields B_{hf}. For T_m=295 K, guidelines from Fig. 2 (preparation at 300 K) are given for comparison (dashed lines). At the right borderline, values for D=21 are given, for the center of the film (——) and for the first layer near an Ag coating (— — —), compare Fig. 2(a). (b) Relative contributions, compare Fig. 2(b), for films coated at T_{Ag}=475 K (○) and T_{Ag}=300 K (⊗), respectively. Layer-growth predictions (solid lines) for comparison.

Magnetic hyperfine fields of components (a)–(d) are shown in Fig. 5(a) for both series, prepared at T_{Fe}=475 K, coated at T_{Ag}=475 K (○,●) and 300 K (⊗), respectively. For T_m=295 K (○,⊗), the guidelines of Fig. 2(a) are included for comparison (dashed lines). It is important that the fields in both new series, prepared at 475 K, can be fitted by the same components as for the previous series, prepared at 300 K, although the higher preparation temperature resulted in a completely different microstructure [compare Figs. 5(b) versus Fig. 2(b)]. This common appearance of the same spectra components under different conditions clearly confirms our structural interpretation of them. B_{hf} measured at T_m=90 K (●) deviates in a reasonable manner from that measured at 295 K: Component (a) becomes completely magnetic with B_{hf}=11 T, as known from previous work of the Ag-coated monolayer.[8] For component (b), the decrease of B_{hf} with decreasing D apparently reflects a thermally induced size effect, which is enhanced by increasing T and decreasing D. For comparison, it has been shown previously[21] that the ground-state value of $B_{hf,b}(0)$=21.7 T is independent of D. Further, $B_{hf,b}$ conveniently converges towards its values for "thick" films (D=21),[6] which are indicated at the right-hand side of Fig. 5(a). Similar situations are observed for components (c) and (d), however, B_{hf} (90 K) increases with decreasing D. This agrees qualitatively with our previous result[6] that for a thick Ag-coated film, $B_{hf}(0)$ in the first monolayer near Ag is enhanced to 35 T, from 34 T in bulk. Apparently, the increase of $B_{hf,d}$ (90 K) with decreasing D is connected with an increasing weight of this Ag-coated top layer in component d. Again, values from "thick" films (D=21)

are given at the right-hand side of the figure, for comparison; subcomponents of (*d*) representing the first monolayer near Ag (— — —) and the center of the $D=21$ film (——) are given separately.

As seen from Fig. 5(a), for films prepared at $T_{Fe}=475$ K, coated at $T_{Ag}=300$ K (⊗), no magnetic subcomponent (*a''*) was observed at $T_m=295$ K in component (*a*). Apparently, the enhanced preparation temperature resulted in a considerable increase in the area of monolayer patches; consequently, the contribution of parts near thicker film patches, which are magnetized by these, becomes negligible. This fits well in our general interpretation of subcomponents (*a'*) and (*a''*). Conversely, for the films coated at $T_{Ag}=475$ K (○), we observed the magnetic component (*a''*) only for $D\geq 1.2$. Apparently, the Ag induced rearrangement results in monolayer patches tightly connected with the thicker ones and magnetized by them.

C. Temperature dependence of hyperfine fields for selected films

The temperature dependence of hyperfine fields $B_{hf,i}$ of different structural components i was measured for temperatures between 90 and 40 K for films consisting of nearly integer numbers of atomic layers. Assuming two basal pseudomorphic layers, these were films near $D=0.82$, 1.64, 2.64, 3.64, etc. As an example, we show in Fig. 7 B_{hf} versus T for components (*b*) and (*c*) in a film W(110)/1.60/Ag [1.60 bulk layers of ^{57}Fe, prepared on W(110), coated by Ag], in comparison with B_{hf} of bulk material. As for the monolayer,[8] we do not find the linear dependence on T which is predicted by the spin-wave theory of the isotropic Heisenberg model in weak external fields, and has been detected previously for the magnetization of NiFe and Co films.[22] We suppose a connection of this deviating temperature dependence with the strong anisotropies in these films, which force the magnetization along the bulk hard axis [1$\bar{1}$0].[19] A theoretically founded ansatz for the temperature dependence is missing. Nevertheless, we fitted the hyperfine fields by $B_{hf}(T)=B_{hf}(0)(1-bT^{3/2})$, in order to get rough values for the ground-state field $B_{hf}(0)$ and some phenomenological parameters b, as a basis for a qualitative discussion of the local structure of thermal decrease and its dependence on D, to be given below. For components (*b*) and (*c*) in Fig. 7, the fit resulted in $\beta=1.31$ and 1.66, respectively. In view of the limited accuracy of the measurements and the limited range of temperatures, the accuracy of β is hardly better than 0.2, and both layers can be described by $\beta=1.5\pm0.2$. In the other films, fitting parameters $\beta=1.5\pm0.2$ were found in a similar way. Accordingly $\beta=\frac{3}{2}$ is suitable for a phenomenological description of the temperature dependence in all films, in a similar manner as in Fig. 7. In their recent study on four atomic layers of Fe(110) in Ag(111), Lugert and Bayreuther[9] also found that $B_{hf}(T)$ could be described by $\beta=\frac{3}{2}$ very well. We therefore used a second fit with $\beta=\frac{3}{2}$, in order to simplify the comparability of the temperature dependence in different films and components, and the comparability with other authors. $B_{hf}(0)$ and b from this second fit, $B_{hf}(T)=B_{hf}(0)(1-bT^{3/2})$, including results from related systems, for comparison, are shown in Table I and discussed in Sec. V.

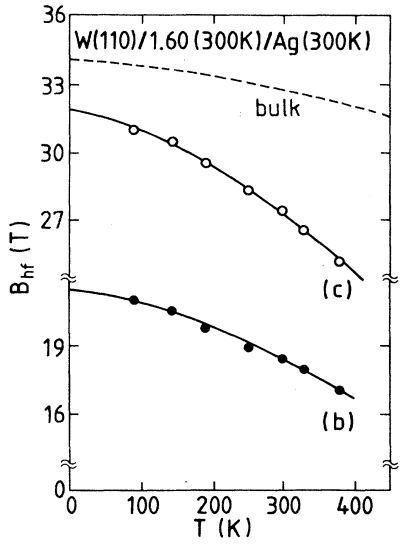

FIG. 7. Magnetic hyperfine field B_{hf} vs T for components (*b*) (first layer) and (*c*) (second layer) in a pseudomorphic double-layer film ($D=1.60$;$\tilde{D}=1.96$), prepared and coated at 300 K. Bulk data are for comparison. The curves are fitted by $B_{hf,b}=21.5$ T $(1-28.1\times10^{-6}\ (T/K)^{3/2})$ and $B_{hf,c}=31.9$ T $[1-28.3\times10^{-6}(T/K)^{3/2}]$, respectively.

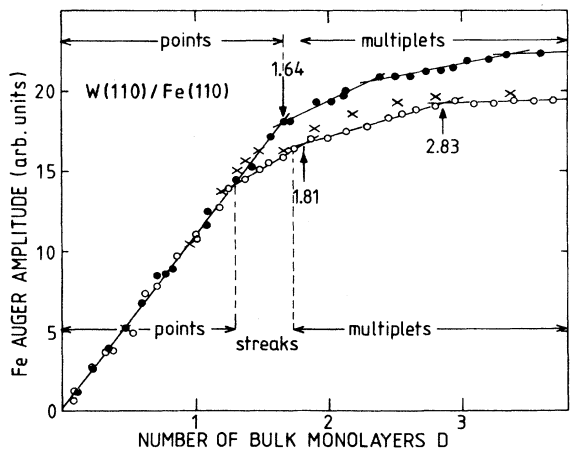

FIG. 8. Fe-Auger-amplitude (47 eV) of Fe(110) films on W(110), prepared at $T_{Fe}=295$ K (●) and $T_{Fe}=475$ K (○, ×), respectively, vs D, the number of bulk monolayers contained in the film. The first kink for $T_{Fe}=295$ K (●) is normalized at $D=1.64$, that means two pseudomorphic monolayers. The structure of the LEED patterns is indicated for (●) and (○). "Points" means a W(110)$p(1\times1)$ pattern; "streaks" are an elongation of these points along [1$\bar{1}$0]. The previously described (Ref. 15) superstructure "multiplets" indicates a two-dimensional network of misfit dislocations.

TABLE I. Fitting parameters $B_{hf}(0)$ and b for the temperature dependence $B_{eff}(T)=B_{hf}(0)(1-bT^{3/2})$ of hyperfine fields $B_{hf}(T)$, for different components in samples consisting of nearly integral numbers of real atomic layers, $\tilde{D}=D+0.36$ (for $D>1.64$). For the notation of sample structure compare sample Nr 5, W(110)/1.65+19/Ag), which means a sample on W(110), consisting of 1.64 bulk layers of ^{57}Fe plus 19 bulk layers of ^{56}Fe, coated by Ag. Data for films on Ag(111) and for bulk Fe for comparison. Samples 1, 2, 3, 5, and 8 were prepared at room temperature, samples 4, 6, and 7 at 475 K. The error for $B_{hf}(0)$ (±0.3 T) relates to $B_{hf}(0)$ as fitting parameter. With respect to the uncertainties in the mode of extrapolation, the error of $B_{hf}(0)$ as a ground-state field is estimated as ±0.5 T, for samples 1–4.

Nr	Sample Structure	d	Component	$B_{hf}(0)$ (T)	b (10^{-6} K$^{-3/2}$)	Reference
			Samples from this paper			
		±0.05		±0.3	±1.0	
1	W(110)/0.82/Ag	1.00	(*a*)	11.7	56.2	This paper
2	W(110)/1.60/Ag	1.96	(*b*)	21.5	28.1	This paper
			(*c*)	31.9	28.3	
3	W(110)/2.55/Ag	2.91	(*b*)	21.0	20.9	This paper
			(*d*)	35.3	20.9	
4	W(110)/5.13/Ag	5.49	(*b*)	21.7	17.0	This paper
			(*d*)	34.8	15.1	
			Further samples, for comparison			
5	W(110)/1.64+19/Ag	21	First layer	21.6	12.9	7
			Second layer	34.3	8.9	
6	W(110)/20+1/Ag	21	Top	34.9	13.3	7
7	W(110)/9+3+9/Ag	21	Central	33.9	6.2	7
8	Ag(111)/4/Ag	4	Interface	35.4	32	9
			Central	33.9	13	
9	Bulk Fe	∞		33.9	5.3	9

IV. LEED AES ANALYSIS

In our previous LEED AES study,[15] we concluded that for preparation at $T_{Fe}=500$ K, the growth of Fe(110) on W(110) starts by two pseudomorphic monolayers. This should be compared with our CEMS results on films prepared at 475 K and coated by Ag at 300 K, which show a slight but distinct deviation from pseudomorphism near $D=1.64$. To clarify this situation further, we performed an additional, more extended, LEED AES analysis in the machine of Ref. 15, with slightly improved vacuum conditions [$p<3\times10^{-10}$ Torr during preparation in comparison with 5×10^{-10} Torr (Ref. 15)] and including preparation both at 475 and 300 K. Results are given in Fig. 8, which shows the Fe-Auger amplitude (47 eV) versus film thickness D and indicates the structure of the LEED pattern. For $T_{Fe}=300$ K, two series of preparations were performed with indistinguishable results, which are therefore represented by one common symbol (●). The Fe amplitude rises linearly up to a first kink, up to which we find only the $p(1\times1)$-W(110) LEED pattern ("points"), that means a pseudomorpic film, whereas just above this kink we observe the previously described[15] superstructure multiplets, indicating periodic misfit dislocations. By comparison with the CEMS results of Sec. III A (Figs. 1 and 2), we identify this first kink with the completion of the second pseudomorphic monolayer ($D=1.64$). It is used for normalization of the D axis. Note that there is definitely no kink at the first monolayer if the Auger analysis is done using a retarding field system [a weak monolayer kink was detected using a cylindrical mirror analyzer (CMA)[16]]. This should be taken as a warning to be cautious if the "monolayer" kink is used for normalization of ultrathin film thickness. We have no explanation for the further two kinks, which are less expressed. For $T_{Fe}=300$ K, two series were performed with only slightly different conditions [(○) with $p<3\times10^{-10}$ Torr (×) with $p<2\times10^{-10}$ Torr, respectively, during preparation]. Nevertheless, there are clear structural differences. For the first series (○), we describe the LEED patterns in the figure and tentatively explain them in the following: The first pseudomorphic monolayer is coated in part by a second one up to $D=1.3$ [linear increase of Fe amplitude, W (1×1) LEED pattern.] Between the first kink at $D=1.3$ and the second at $D=1.81$, the second layer is completed and filled to bulk density, starting in one dimension only, as indicated by streaks along $[1\bar{1}0]$. The third kink at $D=2.83$ shows the completion of the third layer. The deviations of the second preparation (×) confirm the instability of the second pseudomorphic monolayer, which was concluded from the CEMS analysis (compare to Fig. 5). Apparently, the deviation from linearity, and therefore the position of the first kink in the Auger plot, depend sensitively on hidden parameters. This is reasonable in view of the instability of the

second pseudomorphic layer and explains the apparent contradiction to the previous study.[15]

V. DISCUSSION

The present mode of Mössbauer analysis of ultrathin film is based on the favorable strong differences in hyperfine fields of different structural components, which are found in Fe(110) on W(110) and allow a straightforward attribution of fields to components, as shown in Fig. 2. As a Mössbauer technique it is restricted to Fe films. Furthermore, its extension to Fe films on other substrates, with less expressed differences in B_{hf}, like Fe on Ag,[9] may be much more difficult. For the present case, it allows atomistic insight in film structure and mode of growth, discussed in Sec. V A, and in the local structure of magnetic order, discussed in Sec. V B.

A. Film structure and mode of growth

The initial stages of growth of Fe(110) on W(110) are governed by the thermodynamic stability of the first pseudomorphic monolayer. This stability is indicated by the high surface energy of the W substrate ($\gamma_W = 2.9\ \mathrm{J\,m^{-2}}$) in comparison with the much lower one of the film material ($\gamma_{Fe} = 2.0\ \mathrm{J\,m^{-2}}$) (for a general discussion of growth-mode criteria in ultrathin films see (Refs. 12 and 13). However, the heavy strain by $-f_{FeW} = 9.4\%$ in this pseudomorphic layer is connected with additional strain energies of the order of $1\ \mathrm{J\,m^{-2}}$, in a harmonic approximation, which might destroy the stability. Because of anharmonicity of interactions, the strain energies are expected to be lower, but they are hard to calculate. Therefore, it is important that the stability of the pseudomorphic monolayer has recently been confirmed[14] using the Curie temperature of monolayer and submonolayer films ($D \leq 0.82$), $T_{c,\mathrm{mono}} = 282$ K, which turned out to be independent both on D and on annealing up to 800 K.

The stability of the first pseudomorphic monolayer is further confirmed by the data of the present study. This is shown in Fig. 6, which gives the monolayer contributions $p_a + p_b$ versus D which invariably follow the hyperbola $(p_a + p_b) = 0.82/D$ (for $D \geq 0.82$) for all the films of the study, independently on the preparation conditions. This means that the pseudomorphic monolayer is stable both in the presence of thicker film patches and in the interface of a thick film. To our knowledge, this phenomenon of "interface pseudomorphism"[23] has not been detected by other methods. The monolayer stability is further confirmed by the analysis of submonolayer films, to be reported elsewhere, for which components other than (*a*) could never be detected. The same stability of the first pseudomorphic monolayer has recently been shown by AES for the case of Fe(100) on W(100).[24]

Beyond $D = 0.82$, film growth and structure depends sensitively on the preparation conditions. For preparation at $T_{Fe} = 300$ K, film growth proceeds by a second pseudomorphic monolayer. In addition, CEMS data of Fig. 2(b) are consistent with further layer growth. The disappearance of component (*c*) at $D \approx 2.8$ actually indicates the formation of a third monolayer with bulk density on the two pseudomorphic layers. However, possible deviations from this three-layer stage are hard to estimate from the CEMS data, and some deviations are certainly indicated by the Auger data in Fig. 8 (the second kink at $D \approx 2.4$). In addition, reduced contrast in the LEED pattern indicates an enhanced level of steps or point defects. Considerable microscopic roughening for $D > 3$ is connected with preparation at $T_{Fe} = 300$ K; for indications of this roughening by CEMS see Ref. 21.

The second pseudomorphic monolayer seems to be metastable, in agreement with stability considerations for anharmonic interactions.[20] Its completion is prevented by preparation at $T_{Fe} = 475$ K, the growth of it is left near $D = 1.3$, as can be seen from both LEED-AES in Fig. 8 and from CEMS of films coated with Ag at $T_{Ag} = 300$ K (⊗) in Fig. 5; note that Ag coating at 300 K leaves the structures undisturbed, as shown by Fig. 2. However, Ag coating at $T_{Ag} = 475$ K strongly disturbs the film structure above the pseudomorphic monolayer, as seen in Fig. 5 from comparison of films coated at 300 K (⊗) and 475 K (○), respectively. Some annealing experiments with uncoated films, above 475 K, showed, with increasing temperature, an increasing tendency to enhance components (*a*) and (*d*) at the expense of components (*b*) and (*c*); that is, to form three-dimensional (3D) nuclei on top of the pseudomorphic monolayer. This tendency to Stranski-Krastanov growth at elevated temperatures is observed for other metals on W(110), too,[13] e.g., Pd on W(110).[25]

For basic research, we are interested in layer-by-layer structures with a low density of point defects in the surface. For their preparation, the following recipe evolves: The pseudomorphic monolayer, being thermodynamically stable, may be prepared at any temperatures. However, if large area monolayer patches are desired for monolayer research in the submonolayer regime, they should be prepared at elevated temperature ($T > 500$ K).[14] If a second pseudomorphic monolayer is desired, preparation should proceed at 300 K. Finally, the preparation temperature should conveniently be raised with increasing D, slowly enough, on the one side, to avoid islanding, and to high enough temperatures, on the other side, to smoothen the surface.

B. Magnetic hyperfine fields

Two aspects of magnetic hyperfine fields B_{hf} are important for the analysis of magnetic ordered materials in general and of ferromagnetic films in particular: First their ground-state values $B_{hf}(0)$ result in common with magnetic moments from the same band-structure calculations;[1] they form a sensitive test of these calculations with the advantage that they can be determined experimentally with high accuracy and with monolayer resolution, as shown above, in conrast to magnetic moments, for which only integral measurements are possible using magnetometry[26] and rough estimates of the local structure by spin-polarized electron methods.[27] It should be emphasized, however, that $B_{hf}(0)$ cannot be taken as a measure of the ground-state magnetic moment $\mu(0)$. For ex-

ample, in an Ag-coated monolayer of Fe(110) on W(110), $B_{hf}(0)$ is decreased to 12 T,[8] whereas $\mu(0)$ is enhanced to 2.5 μ_B.[28] Secondly, the temperature dependence of $B_{hf}(T)$ can be taken, to a good approximation, as a measure of the temperature dependence $\mu(T)$. In this sense only of a common temperature dependence, $B_{hf}(T)$ can be taken as a local probe of $\mu(T)$. For bulk Fe, the deviation from proportionality between $B_{hf}(T)$ and $\mu(T)$ is below 0.5% for $0 \leq T \leq 300$ K.[29] For the case of ultrathin films, its validity for 90 K $\leq T \leq 300$ K has been shown recently[9] for the case of Fe(110) films in Ag(111). This proportionality of $B_{hf}(T)$ to $\mu(T)$ is reasonable because all contributions to $B_{hf}(T)$ are caused by $\mu(T)$ and therefore should scale with it. However, some reservations must be made with respect to the local resolution of the method, because $B_{hf}(T)$ contains, beside strictly local terms from core polarization and from 3D orbital moments, a nonlocal contribution of the order of 50 T (Ref. 1) from Fermi contact interaction with the spin-polarized conduction-electron gas. Corrections from this mechanism to the local proportionality of $\mu(T)$ and $B_{hf}(T)$ remain to be discussed quantitatively. We suppose, however, that these are minor corrections only, so that $B_{hf}(T)$ basically remains to be used as a measure of $\mu(T)$.

As shown above, the temperature dependence of $B_{hf}(T)$ can be described, for all components of our film, to a reasonable approximation, by a phenomenological Bloch-like ansatz $B_{hf}(T)=B_{hf}(0)(1-b\ T^{3/2})$. This is surprising because spin-wave calculations predict a linear dependence of $\mu(T)$ on T,[22] for isotropic Heisenberg films, and this behavior has been previously observed in several other ultrathin film systems.[22] There are theoretical indications that nonlinear thermal decrease can be induced by strong magnetic anisotropies[30,31] which certainly are present in our films[32] as magnetic surface anisotropies and supposedly cause this nonlinear thermal decrease. It should be emphasized, however, that a strict validity of a $T^{3/2}$ law is not claimed and that low-temperature measurements for a quantitative analysis of $B_{hf}(T)$ are definitely needed.

Nevertheless, parameters b can serve as a phenomenological measure of the strength of thermal decrease. The main information of the CEMS analysis with respect to the magnetism of these ultrathin films is contained in the parameters $B_{hf}(0)$ and b for different components, mainly for films consisting of integer numbers of real atomic layers, $\tilde{D}=1$, 2, 3, 4 ($D=0.82$, 1.64, 2.64, 3.64 bulk monolayers). These data are shown in Table I; data on some related systems are included. We further discuss the table in the following.

(1) $B_{hf}(0)$ of the first monolayer, which we know to be pseudomorphic independently of D, is reduced to 11.7 T in the monolayer film ($D=1.0$, sample 1); it is increased to 21.5±0.5 T if this first monolayer is coated by further Fe [component (*b*)], independently of D, for $D \geq 1.64$ ($D \geq 2$).

(2) $B_{hf}(0)$ in the second monolayer, when forming a part of thick films (sample 5, second layer), is enhanced above its bulk value (33.9 T) to 34.3 T, whereas it is reduced to 31.9 T (sample 2, component *c*) when coated by Ag, as part of a double layer. This is contrary to the surface of a thick Fe(110) film, where coating by Ag results for the topmost layer in an enhancement to $B_{hf}(0)=34.9$ T. Accordingly, the quantitative discussion of the Ag coating on the double layer must be done independently of that on the bulk surface.

(3) $B_{hf}(0)$ for component (*d*), in samples 3 and 4, is enhanced to 35.3 (34.8) T even above its value for the bulk surface (34.9, sample 6); this behavior can be seen in Fig. 5, where B_{hf} (90 K) of component (*d*) is enhanced above its surface value for $D=21$. It is in agreement with the findings of Lugert and Bayreuther[9] on the interface component of four layers Fe(110) in Ag(111), sample 8 in Table I.

(4) Parameters b of the thermal decrease are homogeneous up to $D=3$; for $D=5.5$, they are enhanced by 13% only in the surface component (*b*) in comparison with the bulk component (*d*). Obviously, the temperature dependence of the different layers is clamped completely up to $D=3$ (approximately to $D=5$) by the strong interlayer exchange coupling. This is in excellent agreement with previous theoretical work of Haubenreisser *et al.*[33] on Fe(100) films, who predicted, for $D=4$, an inhomogeneity at the moment of less than 1% (4%) for $T \leq 300$ K ($T \leq 500$ K). Similar behavior was predicted recently for Ni(100) by Hasegawa.[33] To our knowledge, the present work forms the first experimental evidence for this clamped temperature dependence.

In sharp contrast, Lugert and Bayreuther,[9] for their four-layer thick Fe(110) film prepared on Ag(111) (sample 8 in Table I), found an enhancement by a factor of 2.5 of the b parameter for the interface component in comparison with the central one. In our opinion, this must be explained based on the microstructure of these films, which became continuous only above three atomic layers,[9] as expected from the surface energies. Apparently, the "interface component" of these Fe(110) films on Ag(111), which nucleate by islands, is coupled much more loosely to the center than in our films on W(110), which, in turn, start growing by a stable monolayer and therefore relate much better to theoretical layer-by-layer models. It should be noted that a similar difference was observed at the surface of epitaxial films of Fe(110) prepared on Ag(111) (Ref. 34) or W(110) (Ref. 6), respectively. The enhancement factor of b in the surface layer was found to be 3.5 for preparation on Ag(111) (Ref. 35) but (2.0±0.2) for preparation on W(110) (Ref. 6) (compare samples 6 and 7 in Table I), the latter result being in agreement with predictions of Rado[35] by spin-wave theory for the case of homogeneous interlayer exchange interaction. Mathon and Ahmad[36] have recently shown how b of the surface layer is enhanced by reduced exchange coupling between the surface layer and following layers. The strong surface enhancement of b in Fe(110) films on Ag(111) therefore indicates weakened exchange coupling in the interface, which supposedly is connected with some loose surface structure, which is not known in detail. Conversely, the homogeneity of b in our Fe(110) films on W(110) can be taken as a magnetic confirmation of their good single crystalline structure.

(5) Parameters b of the double layer ($D=2$) are half that of the monolayer ($D=1$), and for $D \leq 5.5$ they scale with $1/D$ to a good approximation. This means that the thermal reduction of the magnetic moment is independent on D. This is what should be expected if (a) the ground-state magnetic moment is the same in the monolayer and in the thicker films and if (b) the spectrum of thermal excitations is independent of D.[22] Condition (a) has been checked recently[28,37] by monolayer magnetometry resulting in weak enhancement only of $(14\pm5)\%$ of the monolayer moment in comparison with that of bulk Fe. Our findings therefore indicate the situation of condition (b), again as a result of rigid exchange coupling.

(6) In our opinion, the experimental determination of $B_{\rm hf}(0)$ in the pseudomorphic monolayer and the pseudomorphic double layer (samples 1 and 2, respectively, both coated by Ag) forms a challenge for band-structure calculations both because of their high accuracy and because of the two-dimensional translational symmetry of the samples.

VI. SUMMARY AND CONCLUSIONS

In conclusion, we have shown that in ultrathin pure ^{57}Fe(110) films on W(110), coated by Ag, different structural components can be distinguished by strongly different magnetic hyperfine fields. Based on this, the initial stages of growth could be followed. The films start by a thermodynamically stable pseudomorphic monolayer, both at room temperature and elevated temperatures (474 K). At room temperature, a second pseudomorphic monolayer is formed followed by flat films with a slightly roughened surface, on an atomic scale. At elevated temperatures, the second pseudomorphic monolayer cannot be realized, but the surface of thicker films becomes atomically smooth. Ag coating should be performed at room temperature to avoid disturbance of the layer structures.

The local structure of thermal decrease of magnetic order was analyzed by CEMS in a series of films consisting of nearly integer numbers of atomic layers, by measuring their CEMS spectra for $90<T<400$ K. Ground-state magnetic hyperfine fields $B_{\rm hf}(0)$ for different components differ strongly from their bulk values; with respect to their local variation, they cannot be taken as a measure of magnetic moments μ. With respect to their temperature dependence, however, magnetic hyperfine fields $B_{\rm hf}(T)$ can be taken as a measure of $\mu(T)$ and therefore can be used to probe the local structure of thermal decrease of $\mu(T)$. Appropriate parameters of the thermal decrease are homogeneous across the film for the very thinnest films (up to five layers), as a result of strong interlayer exchange coupling.

ACKNOWLEDGMENTS

This work was supported in part by the Stiftung Volkswagenwerk.

*Permanent address: Solid State Physics Department, Academy of Mining and Metallurgy, Krakow, Poland.

[1]A. J. Freeman and C. L. Fu, J. Appl. Phys. **61**, 3356 (1987).
[2]W. Haubenreisser, W. Brodkorb, A. Corciovei, and G. Costache, Phys. Status Solidi **31**, 245 (1969).
[3]J. Tyson, A. H. Owens, J. C. Walker, and G. Bayreuther, J. Appl. Phys. **52**, 2487 (1981).
[4]J. Korecki and U. Gradmann, Phys. Rev. Lett. **55**, 249 (1985).
[5]J. Korecki and U. Gradmann, Hyperfine Interact. **28**, 931 (1986).
[6]J. Korecki and U. Gradmann, Europhys. Lett. **2**, 651 (1986).
[7]M. Przybylski, U. Gradmann, and J. Korecki, J. Magn. Magn. Mater. **69**, 199 (1987).
[8]M. Przybylski and U. Gradmann, Phys. Rev. Lett. **59**, 1152 (1987).
[9]G. Lugert and G. Bayreuther, Phys. Rev. B **38**, 11 068 (1988).
[10]N. C. Koon, B. T. Jonker, F. A. Volkening, J. J. Krebs, and G. A. Prinz, Phys. Rev. Lett. **59**, 2463 (1987).
[11]L. Z. Mezey and J. Giber, Surf. Sci. **117**, 220 (1982).
[12]E. G. Bauer, Z. Kristallogr. **110**, 372 (1958).
[13]E. Bauer and J. H. van der Merwe, Phys. Rev. B **33**, 3657 (1986).
[14]M. Przybylski and U. Gradmann, J. Phys. (Paris) C **8**, 1705 (1988).
[15]U. Gradmann and G. Waller, Surf. Sci. **116**, 539 (1982).
[16]T. M. Gardiner, Thin Solid Films **105**, 213 (1983).
[17]M. Przybylski and U. Gradmann, J. Appl. Phys. **63**, 3652 (1988).
[18]For a standard representation of Mössbauer analysis compare N. N. Greenwood and T. C. Gibb, *Mössbauer Spectroscopy* (Chapman and Hall, London, 1971).
[19]U. Gradmann, J. Korecki, and G. Waller, Appl. Phys. A **39**, 101 (1986).
[20]A. Milchev and I. Markov, Surf. Sci. **136**, 503 (1984).
[21]M. Przybylski and U. Gradmann, Hyperfine Interact. **41**, 693 (1988).
[22]U. Gradmann, Appl. Phys. **3**, 161 (1974).
[23]M. Przybylski and U. Gradmann, in *The Structure of Surfaces II*, edited by J. F. van der Veer and M. A. van Hove (Springer-Verlag, Berlin, 1988).
[24]X. L. Zhou, Y. C. Yoon, and J. M. White, Surf. Sci. **203**, 53 (1988).
[25]W. Schlenk and E. Bauer, Surf. Sci. **116**, 313 (1982).
[26]U. Gradman, R. Bergholz, and E. Bergter, Thin Solid Films **126**, 107 (1985).
[27]*Polarized Electrons in Surface Physics*, edited by R. Feder (World Scientific, Singapore, 1985).
[28]H. J. Elmers and U. Gradmann, Phys. Rev. Lett. **63**, 566 (1989).
[29]I. Vincze and J. Kollar, Phys. Rev. B **6**, 1066 (1972).
[30]J. A. Davis, J. Appl. Phys. **36**, 3520 (1965).
[31]J. C. Levy and J. L. Motchane, J. Vac. Sci. Technol. **9**, 721 (1972).
[32]H. J. Elmers and U. Gradmann, J. Appl. Phys. **64**, 5328 (1988).
[33]H. Hasegawa, Surf. Sci. **182**, 591 (1987).
[34]G. Stern, G. N. Sapir, and J. C. Walker, J. Magn. Magn. Mater. **54-57**, 799 (1986).
[35]G. J. Rado, Bull. Am. Phys. Soc. **2**, 127 (1957).
[36]J. Mathon and S. B. Ahmad, Phys. Rev. B **37**, 660 (1988).
[37]U. Gradmann, H. J. Elmers, and M. Przybylski, J. Phys. (Paris) C **8**, 1665 (1988).